*Proceedings of the*
*Annual Stability Conference*
*Structural Stability Research Council*
*Atlanta, Georgia, April 21-24, 2020*

# Analysis of non-symmetric cross-sections relative to the provisions of AISC 360-10

Edward J. Sippel[1], Ronald D. Ziemian[2], Hannah B. Blum[3]

**Abstract**
Non-doubly symmetric sections are used for a variety of applications that range from the main member of a large portal frame to angles framing small roof penetrations in steel structures. These non-doubly symmetric sections challenge the structural analysis process with more complex displacements and stability limits compared to doubly symmetric sections due to non-concentric shear centers and centroids. This project investigated the response identified by a structural analysis that meets the current analysis requirements of the AISC specification and assumes doubly symmetric cross sections versus an analysis that more accurately models non-doubly symmetric cross section information. Beam finite element models were created in multiple structural analysis programs to perform this evaluation. The results were compared to shell-element models created in Abaqus and experimental results when available. The modeling processes used were verified to meet the design requirements of the Direct Analysis Method and Advanced Analysis Method. These procedures were used to model three single member examples that included non-doubly symmetric cross sections to compare the calculation of displacements and stability limits. Finally, a mono-symmetric I-beam portal frame was evaluated to consider the impact of sharing forces within a system.

## 1. Introduction

The Direct Analysis Method was introduced in the 2005 AISC Steel Specification (AISC 2005) as an alternative method to design steel structures of all frame types and sections (Griffis & White 2013) from the Effective Length Method that had previously been the industry standard. Chapter C of the 2016 AISC Steel Specification (AISC 2016) lists the current requirements to follow the Direct Analysis Method. The Direct Analysis Method encompasses a full design approach that allows the engineer to complete one type of structural analysis and assess those force distributions with a specific set of design requirements. The provisions of the Direct Analysis Method indicate that the analysis needs to consider flexural, shear, axial, and all other component deformations that contribute to the displacement of the structure. The analysis must also consider the effects of $P$-$\delta$ and $P$-$\Delta$ for the structure. The Direct Analysis Method has no

[1] Graduate Research Assistant, University of Wisconsin-Madison, <esippel@wisc.edu>
[2] Professor, Bucknell University, <ziemian@bucknell.edu>
[3] Assistant Professor and Alain H. Peyrot Fellow, University of Wisconsin-Madison, <hannah.blum@wisc.edu>

requirements for the inclusion of torsion and second order twisting effects. The consideration of these effects and the determination if they would have a significant influence on structural performance is left to the discretion of the engineer. A structure composed of doubly symmetric sections such as standard I-beams and HSS members will have negligible twisting effects if the members are loaded in a single plane and do not have eccentricity out of that plane. However, if either of those conditions is not met these doubly symmetric sections will begin to twist and this can lead to significantly different results as discussed by Ziemian et al. (2018). The use of non-doubly symmetric sections such as channels, angles, and tees further complicates this issue. These cross sections have a nonconcentric centroid and shear center, which means an applied load may cause a resulting torsion and cause the cross section to begin to move out of plane even when the load appears centered on the section.

In addition to the decisions made by the engineer as to what is critical to include, the engineer is often limited to the abilities of the structural analysis software available to them. Many structural analysis programs utilize a beam (line) element that assumes a doubly symmetric cross section with six degrees of freedom per end of the element regardless of the actual shape. Non-doubly symmetric cross sections are allowed to be used within these programs, but limitations exist. The underlying mechanics of the members are typically assumed to still behave the same as a doubly symmetric section. The consideration of what effect the nonconcentric shear center and centroid have is left to the user to decide the appropriate alterations to make to a typical model with some direction from design guides, help forums, and experience. Recent work by Liu et al. (2018, 2019) defined a new line element that removes the doubly symmetric assumption and directly accounts for the different behavior of non-doubly symmetric sections. This element has been implemented into MASTAN2 (Ziemian et al. 2019) with additional tools to readily model non-doubly symmetric sections.

In this paper an initial comparison of the different results from the structural analysis of non-doubly symmetric sections is presented. The focus of the study was on comparing how an analysis approach that would meet the requirements as part of the Direct Analysis Method would be different when working with a method that treated all sections as doubly symmetric versus one that includes behavior related to asymmetry. The project started by focusing on the mechanical responses that were required to be included as part of the Direct Analysis Method. After observing how single non-doubly symmetric members behave, the project then proceeded to evaluate a system of singly symmetric cross sections in a model following the Direct Analysis Method. The objective of this study is to highlight locations where and what type of discrepancies can exist.

## 2. Structural Analysis Utilized

Many different options and methods are available to engineers to complete their structural analysis. A common approach for practicing engineers is to use a commercially available structural analysis program that implements a line element that assumes a doubly symmetric cross section. This project included results from both SAP2000 (CSI America 2018) and RFEM (Dlubal Software 2012) to represent this possibility. Another approach would be to utilize a method that does not assume doubly symmetric. One method available within many structural analysis programs would be to use shell or solid elements to build the model. This was considered for this project using Abaqus (Dassault Systems 2015b) to create shell element

models for each problem. However, even a small structure modeled this way would become unwieldly quite quickly; therefore a line element model that removes the doubly symmetric assumption would be an alternative to not substantially change from common current modeling procedures. This project chose to employ MASTAN2 (Ziemian et al. 2019) and Abaqus as two programs that allow for the inclusion of asymmetric properties while using line elements. When identifying the results in tables and graphs, line element models will be identified by the program name and the shell element model in Abaqus will be identified by the label "shells".

*2.1 Analysis for the Direct Analysis Method*

The Direct Analysis Method is one design procedure alternative to follow for the design of a steel building structure. The method requires a structural analysis meeting specific requirements to follow different design rules. Some analysis requirements direct the actions of the user, while a few other provisions indicate the minimum requirements of the structural analysis method or program. It was determined to verify that each program used could model the effects of flexural and axial deformations in addition to *P-δ* and *P-Δ* considerations. The verification was completed by following the example problems provided in the AISC commentary (AISC 2016) and an indeterminate example from the referenced design guide (Kaehler et al. 2011). The three beam problems solved are shown in Figure 1 and also list the common parameters used. Example beam 1 verifies the inclusion of both *P-δ* and *P-Δ* effects while beam 2 and beam 3 highlight just the *P-δ* effects in a member. Example beam 3 was included to verify that the convergence study within each program was not being artificially lowered due to the problem symmetry.

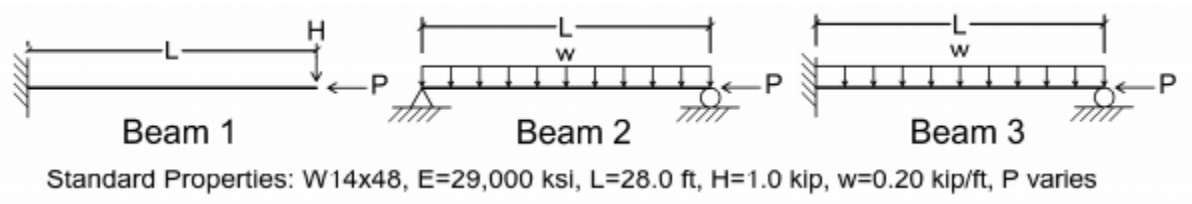


Figure 1: Direct Analysis Method Verification Problems

A model for each problem from Figure 1 was built within each program utilizing the line elements. The programs of SAP2000, RFEM, and MASTAN2 have one option to choose for a frame element supporting moments and axial force, but additional features of the element in MASTAN2 could be included based on the properties defined and boundary conditions including warping and asymmetric considerations. The line element used in Abaqus was the two-node three dimensional open section that included warping, B31OS (Dassault Systems 2015a), integrated during the analysis. For the verification problems, the section properties of the W14x48 were taken from program provided AISC-based tables for SAP2000, RFEM, and MASTAN2. In Abaqus, there were alternatives to use a generic cross section where the same identical section property information could be assigned; however, as the integration feature during analysis was used the dimensions were needed to be provided to allow Abaqus to calculate the section properties and other necessary information itself. The mesh of these models was varied from 2 elements to 64 elements using a factor of 2 along the length of the member resulting in elements varying from 168 inches to 5.25 inches. The loading was applied as distributed loads on members and discrete point loads on nodes at the locations indicated in Figure 1.

A model consisting of shell elements was also created in Abaqus for each problem. A shell element model was chosen since a cross section effective length to thickness ratio of 3 or larger could be captured by a thick or thin shell mechanical response (Akin 2010). The shell models utilized the S4R shell element that has a 4 node linear formulation with reduced integration, hour-glass control, and a general formulation that includes both the thick and thin shell behavior (Dassault Systems 2015b). The I-beam members consisted of three planes of elements attached together to form the complete section as illustrated in Figure 2. The section was defined with an overall height equal to the web and with top and bottom flanges offset to the edge of the element to model the full cross section without overlap as shown below. The full member was meshed based on a single seed value to have consistent sized, approximately square elements along the full length. The largest seed value of 4 inches was based on half of the flange width which was decreased for the mesh study by factors of 2 until there were 128 elements across a single flange. Since none of the Direct Analysis Method verification problems shown in Figure 1 were altered by having free or fixed warping end conditions, the end nodes of all members were rigidly tied together which fixed warping and allowed for boundary conditions and point loads to be applied at a single reference node. Distributed loading was applied as a series of point loads at all nodes on the neutral axis of the member based on the tributary length of the elements.

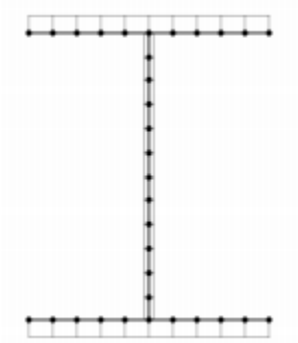

Figure 2: Shell Model Offsets in I-Beam

All of the structural analysis programs considered were able to solve the Direct Analysis Method verification problems. Since the solution trends were similar among all three problems, only the solution to Beam 3 will be discussed in detail. The analytical solution was provided in Design Guide 25 (Kaehler et al. 2013) and follows in Eq. 1 through Eq. 4.

$$\Delta = \frac{wL^4}{192EI}\left[\frac{6}{u^4}\left[(2\sec u - u^2 - 2) - \frac{(\tan u - u)(\sec u - 1)}{\frac{1}{2u} - \frac{1}{\tan 2u}}\right]\right] \tag{1}$$

$$M = \frac{wL^2}{8}\left[\frac{2(\tan u - u)}{u^2\left(\frac{1}{2u} - \frac{1}{\tan 2u}\right)}\right] \tag{2}$$

$$u = \frac{\pi}{2}\sqrt{\frac{P}{P_{eL}}} \tag{3}$$

$$P_{eL} = \frac{\pi^2 EI}{L^2} \tag{4}$$

where $E$ is the modulus of elasticity, $I$ is the moment of inertia, $L$ is the length, $P_{eL}$ is the elastic buckling load for a simply supported beam, $P$ is the applied axial load, $w$ is the applied

distributed load, $M$ is the moment reaction at the support, and $\Delta$ is the beam deflection at midspan. Table 1 summarizes the calculated results to beam 3 from the analytical solution and each program at the finest mesh size modeled.

Table 1: Analysis Results of Beam 3: A Propped Cantilever

| Program | Analytical | SAP2000 | RFEM | MASTAN2 | ABAQUS | Shells |
|---|---|---|---|---|---|---|
| $P$ (kip) | Vertical Displacement at Midspan, $\Delta$ | | | | | |
| 0 | 0.079 | 0.084 | 0.085 | 0.084 | 0.085 | 0.086 |
| 300 | 0.089 | 0.096 | 0.096 | 0.096 | 0.096 | 0.098 |
| 600 | 0.103 | 0.111 | 0.111 | 0.111 | 0.112 | 0.114 |
| 900 | 0.121 | 0.132 | 0.133 | 0.132 | 0.133 | 0.136 |
| 1200 | 0.148 | 0.165 | 0.165 | 0.164 | 0.166 | 0.169 |
| $P$ (kip) | Support Moment, $M$ | | | | | |
| 0 | 235 | 234 | 233 | 234 | 234 | 234 |
| 300 | 257 | 257 | 256 | 257 | 257 | 257 |
| 600 | 284 | 287 | 286 | 287 | 287 | 288 |
| 900 | 322 | 328 | 327 | 328 | 328 | 330 |
| 1200 | 375 | 389 | 388 | 389 | 389 | 393 |

It can be seen that the program solutions are very consistent, but do not match the analytical solution exactly. The analytical solution accounted for bending deformation due to the axial and lateral loading. However, the solution from each of the structural analysis programs accounts for shear deformations and the effects of axial compression. This difference was previously observed in the first two beams shown in Figure 1 and resulted in the updated reference values provided in the AISC 2016 commentary (AISC 2016) that do not exactly match the analytical solution shown in previous editions (AISC 2005, AISC 2010), but include the effects of bending, shear deformations, and axial compression similar to the results in Table 1.

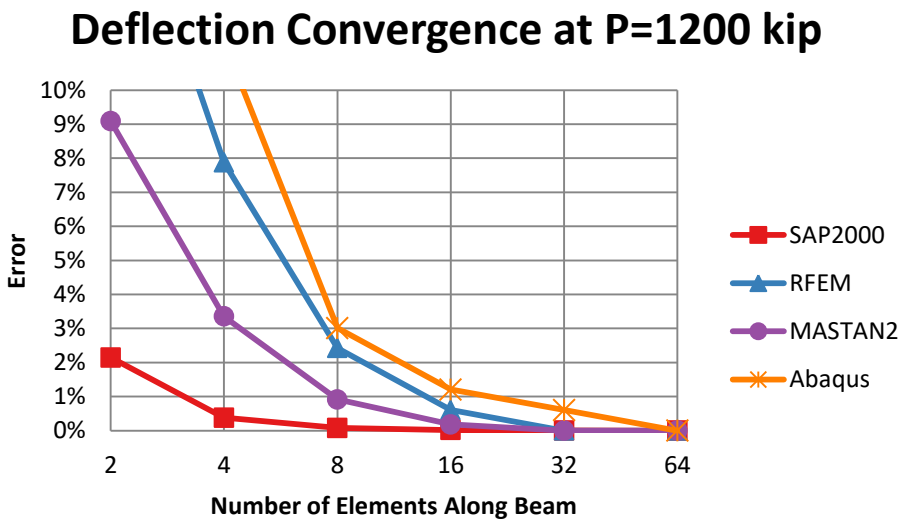


Figure 3: Deflection Convergence for Beam 3

The convergence of the solutions varied both across structural analysis programs and with the applied axial load. When a small axial load was applied, the analysis displayed little nonlinearity and converged rapidly with minimal meshing. As shown in Figure 3 and Figure 4, it was found that at a large axial load with nonlinearity required a finer mesh size to accurately solve the

problem. It was found the analyses were exhibiting less than a 1% change to the solution when using a mesh size of at least 32-10.5 inch long elements per member. The shell element model was excluded from these figures as the number of elements across the cross section was not sensitive in this analysis. The use of an approximately square mesh size caused even the coarsest mesh size with a seed length of 4 inches to have 84 elements along the length of the beam. The results were indicating quick convergence of the solution since the problems in Figure 1 do not include variation in the stress across the width of the flange unlike the remaining problems in this analysis.

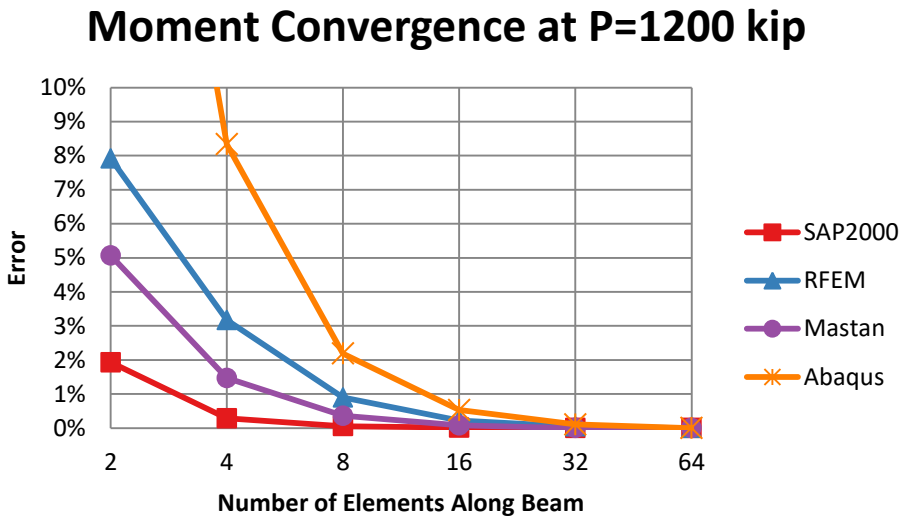


Figure 4: Moment Convergence for Beam 3

*2.2 Advanced Analysis Options*

A structural analysis method that meets the requirements of an analysis as part of the Direct Analysis Method is only required to meet the previously mentioned requirements in a two-dimensional analysis. Additional checks were completed with each structural analysis program to assess the ability to include out of plane rotations, warping, twisting effects, and non-doubly symmetric sections. The ability of the programs to transmit moments through corners with rotations was assessed using a right angle frame shown in Figure 5(a), which was experimentally tested by Spillers et al. (1993) and had a Young's modulus of 10,800 ksi and Poisson's ratio of 0.35. This frame is similar to the one used by Argyris et al. (1979) and discussed by McGuire et al. (2001). The structural analysis program is only capable of obtaining an accurate solution when accounting for the effects of finite rotations at the corner as excluding this term finds a substantially lower buckling mode. The warping and twisting effects were evaluated using the example problem for advanced analysis from the AISC Steel Specification Appendix 1 commentary (AISC 2016) shown in Figure 5(b). The problem is evaluated at 0.8 times the Young's Modulus with typical properties of $E$ = 29000 ksi and $\nu$ = 0.30 and has an initial lateral displacement equal to $L$/1000. The provided solution was evaluated without shear deformation. The displacement response and resulting final equilibrium position was found to be quite different based on whether or not the structural analysis program includes warping and/or secondary twist effect making it possible to discern the type of analysis completed. Finally, a cantilevered monosymmetric I-beam was loaded with point loads in all three principal directions to identify variations from a typical doubly symmetric beam response.

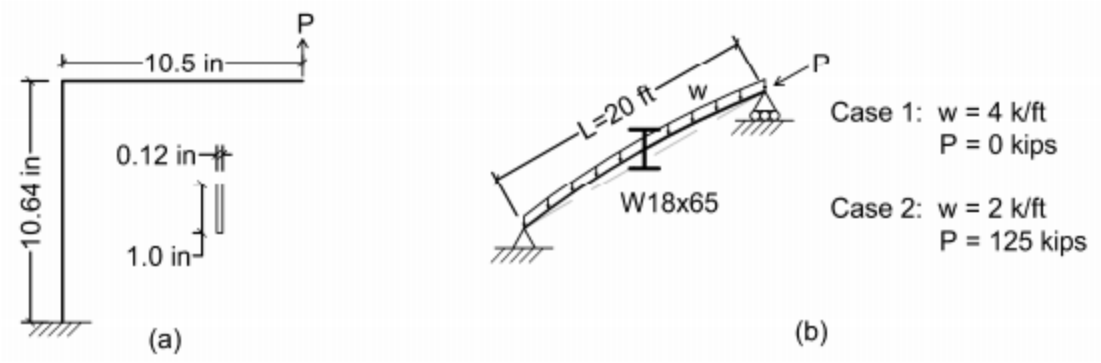


Figure 5: Advanced Analysis Verification Problems

When evaluating the frame from Spiller and the AISC example problem, it was found that not all structural analysis procedures could obtain the correct solution. A solution that evaluated the initial *P-δ* effects alone would not be able to capture an accurate result. Finding an accurate result to these problems required evaluating the equilibrium of the structure in the deformed configuration.

The frame from Spiller has a first failure mode of lateral torsional buckling. The frames were loaded with the vertical load and a small lateral load of 0.001 lb at the tip concurrently to add an imperfection to the model. The superposition of these loadings alone would miss the torsion of the horizontal arm and weak axis moment about the column which could hide the instability. When the problem was reevaluated in the updated equilibrium position it was observed that the lateral displacement of the knee of the frame would rapidly increase thus indicating buckling. The experimental testing by Spiller observed a buckling load of approximately 25 lbs. The programs used for this project all exhibited a buckling failure between 22.7 lbs to 26.8 lbs. This range was deemed acceptable based on the variability in defining an exact buckling load. The effort of defining buckling was complicated by a stable post buckling response that included an increasing maximum displacement which was sensitive to the applied imperfection. Efforts were made to have similar total displacement at the final loading, but some variation still existed.

Table 2: Advanced Analysis Example Solution

| | Analysis Type | $M_{ux}$ (k-ft) | $M_{uy}$ (k-ft) | $\delta_y$ (in) | $\delta_x$ (in) | $\theta$ (rad) |
|---|---|---|---|---|---|---|
| Case 1 | Without Warping | 2386 | 258 | 0.694 | 0.967 | 0.1078 |
| | Including Warping | 2399 | 55.8 | 0.589 | 0.214 | 0.0233 |
| Case 2 | Without Warping | 1235 | 192 | 0.342 | 0.833 | 0.0471 |
| | Including Warping | 1237 | 140 | 0.318 | 0.616 | 0.0266 |

The AISC example problem allowed for the verification of the displacements and forces calculated in an analysis with a member experiencing second order twist effects. The inclusion of a problem that has twisting required the identification of whether warping is included. The effects of warping make the member stiffer in torsion resulting in smaller rotations and when considering second order twist effects smaller displacements, as summarized for this problem in Table 2. Provided in the table are the moments in the rotated equilibrium orientation, $M_{ux}$ about the strong axis and $M_{uy}$ about the weak axis, as well as the vertical displacement $\delta_y$, horizontal displacement $\delta_x$, and the rotation $\theta$ at the middle of the member. While the solution for the major

axis moment did not substantially change, the remaining components of the solution are significantly different.

The inclusion of warping is not a commonly found structural analysis feature. Most programs do not include it as an option because the analysis is often deemed to be conservative when ignoring warping. Both SAP2000 and RFEM were used to run an analysis without warping on an assumed doubly symmetric cross section. There was a module within RFEM that allowed for the analysis of part of a structure including warping, but that was not utilized for this project except where explicitly stated. The inclusion of warping was considered in both MASTAN2 and Abaqus. While options exist within both programs to ignore warping, the behavior of non-doubly symmetric sections exhibit warping behaviors that cause important effects that were to be considered in the following stages of this project. This caused the solutions from each program to be grouped into two distinct responses as shown in Table 3.

Table 3: Advanced Analysis Example Results

| Program | SAP2000 | RFEM | MASTAN2 | ABAQUS | Shells |
|---|---|---|---|---|---|
| | Without Warping | | Including Warping | | |
| | Case 1 | | | | |
| $M_{ux}$ (k-ft) | 2386 | 2386 | 2389 | 2398 | 2398 |
| $M_{uy}$ (k-ft) | 258 | 258 | 73 | 57 | 67 |
| $\delta_y$ (in) | 0.694 | 0.692 | 0.589 | 0.624 | 0.629 |
| $\delta_x$ (in) | 0.968 | 0.967 | 0.213 | 0.22 | 0.262 |
| $\theta$ (rad) | 0.1079 | 0.1079 | 0.0231 | 0.0238 | 0.0280 |
| | Case 2 | | | | |
| $M_{ux}$ (k-ft) | 1235 | 1234 | 1235 | 1237 | 1238 |
| $M_{uy}$ (k-ft) | 193 | 191 | 144 | 143 | 153 |
| $\delta_y$ (in) | 0.342 | 0.340 | 0.316 | 0.337 | 0.343 |
| $\delta_x$ (in) | 0.835 | 0.823 | 0.588 | 0.632 | 0.675 |
| $\theta$ (rad) | 0.0472 | 0.0467 | 0.0242 | 0.0275 | 0.0313 |

The results from each program match reasonably well with the anticipated results. The analysis completed in SAP2000, RFEM, and MASTAN2 were all done without the considerations of shear deformations and using AISC provided section properties to best match the tabulated values. The analyses in Abaqus, both the shell element and line element models, were completed with the consideration of shear deformations and ignoring fillets. While this did introduce a discrepancy from the tabulated solution for these models, this decision allowed for better comparison for the shell element model as it was not possible to ignore shear deformations in that method of evaluation. The results from SAP2000 and RFEM were nearly identical with only minor variations in the lateral displacement and twist under the presence of axial loading. The evaluations with warping included did have a bit more variability as expected. The solution from MASTAN2 was closest to the tabulated values with a conservative weak axis moment being the greatest discrepancy. The values from Abaqus exhibited slightly larger deformations due to shear deformations. The use of a generic section for the line element model in Abaqus did require an overlap of the web and half the flange thickness at both ends, but this resulted in a reasonable approximation for the impact of fillets on the analysis. The shell element analysis was found to have slightly larger results than all previous analyses, but closely followed the trends from the Abaqus line element analysis results. Overall, all methods and programs were able to obtain results that could capture the second order twist effects.

The observed convergence of the line element models did not change substantially when introducing the twisting effects. However, the convergence of the shell element model changed from the Direct Analysis Method verification problems. The advanced analysis problems introduced variations in the stress across the flanges that required a significantly greater number of elements to minimize error. The advanced analysis example had increased convergence requirements with the largest variation observed in Case 2 and are shown in Figure 6. The strong axis moment and vertical deflection were found to have errors that quickly decreased, but the overall lateral displacement of the cross section required many more elements to converge. The analysis was completed with a maximum of 128 elements across the flange of the I-beam using a mesh seed size of 0.0593 in. For the completed analysis to only have a 1% difference compared to that solution at least 32 elements across the flange which equates to a mesh seed size of 0.237 in were needed. As a result, the remaining evaluations in this project were completed with at least that number of elements across the extreme flange.

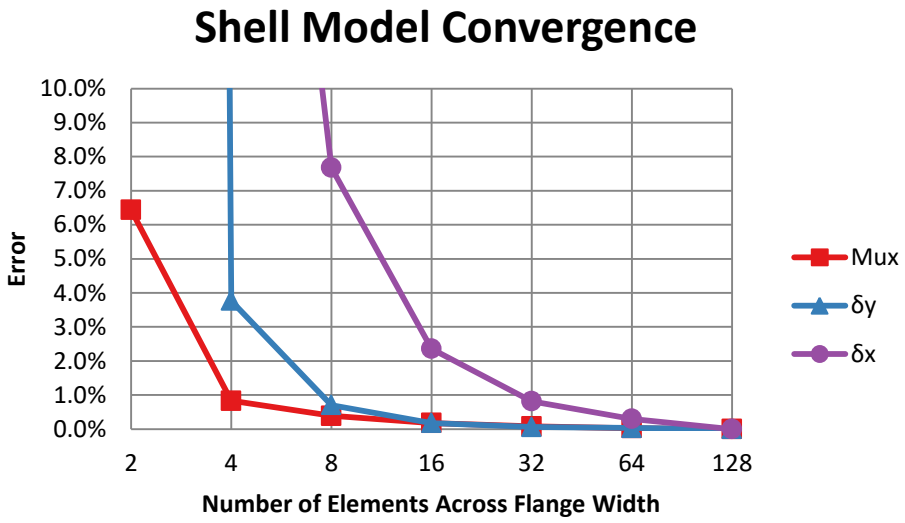


Figure 6: Shell Element Model Convergence in Case 2 of the Advanced Analysis Example

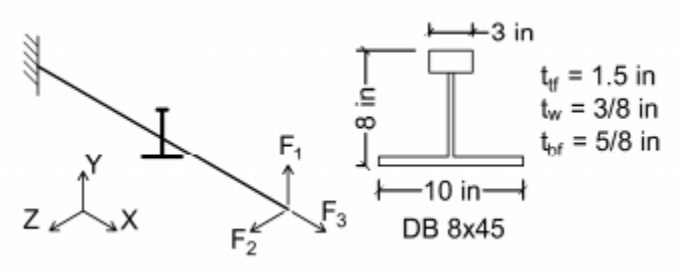


Figure 7: Mono-symmetric I-beam Cantilever

The evaluation of the cantilevered mono-symmetric I-beam shown in Figure 7 consistently found that the commercially available programs treated the members the same as doubly symmetric sections. The load was applied to the member with considerations of rigid links from the end node to the centroid of the cross section. Programs defaulted to the input node being at the centroid location. User documentation provided guidance to the engineer to keep the cross section centered at the centroid and to add any additionally necessary moment to the section (Dlubal Software 2019) or to offset the member such that the input node is the shear center to

automatically include torsional effects from transverse loads (CSI America 2014). These methods worked to achieve the desired loading effects when applied appropriately, but each had limitations such as accidentally applying a moment from applying $F_{3,}$ a pure axial loading, while using offsets. There was an exception observed in SAP2000 that automated some of the considerations of the offset shear center for certain situations, but those features were not utilized for the models used in this project. It was possible to obtain the singly symmetric responses in MASTAN2 and Abaqus. MASTAN2 treated the end node as the centroid of the cross section and added in appropriate moments from only the transverse shear $F_2$ as desired. The line element models created in Abaqus utilized a generic cross section which allowed any location to be picked as the reference node for the member. Applying loads at the centroid required the inclusion of a rigid link from the centroid to the reference node on the cross section which for this analysis was defined as the shear center. The user documentation indicated the choice of this location was arbitrary (Dassault Systems 2015b) and initial evaluations found the use of the shear center was able to consistently solve the initial problems.

## 3. Member Modeling

The work by Liu et al. (2018, 2019) has shown that MASTAN2 with recent improvements is capable of solving problems with a non-doubly symmetric cross section. These problems captured various responses that cannot be found by typical doubly symmetric structural analysis procedures. Rather than repeating these models within the other structural analysis programs to obtain a baseline comparison, three new single member problems were considered. These problems presented additional member responses that would not occur within doubly symmetric members, but would be exhibited by non-doubly symmetric members.

### *3.1 Pure Torsion on an Angle*

A single member subjected to equal and opposite end torques is one of the simplest twisting problems that can be solved. Even when the ends of the member are free to warp the introduction of noncircular sections introduces warping and resulting deformations. A simple example of a standard I-beam section would result in a member that twists about the concentric shear center and centroid and results in an overall shortening as to not cause a net tension (Attard 1986). This problem is further complicated in a non-doubly symmetric section as the location of the shear center moves laterally as shown by Gregory (1960) for an equal angle. Gregory utilized equilibrium of the cross section to calculate the movement of the shear center which was validated by experimental results. Attard (1984) found a similar relationship for non-doubly symmetric sections using nonlinear torsion theory. Eq. 5 and Eq. 6 define the movement of the shear center of a singly symmetric section which is equivalent to the equations found by Gregory when assuming a thin-walled equal angle cross section.

$$v = \beta_1/2(1 - cos\phi) \tag{5}$$

$$w = \beta_1/2(\phi - sin\phi) \tag{6}$$

where $v$ is the displacement parallel to the plane of symmetry, $w$ is the displacement in perpendicular to the plane of symmetry, $\beta_1$ is the Wagner coefficient, and $\phi$ is the total twist of the section. This equation is slightly different from the one presented by both Gregory and Attard due to the definition of $\beta_1$ being updated to match the formulation used by MASTAN2 and CUFSM.

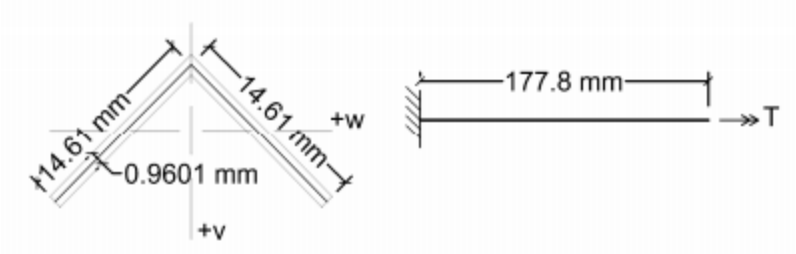

Figure 8: Equal Angle Subjected to Pure Torsion

The model was based on the experiment completed by Gregory (1960) where an equal angle, brass member was subjected to pure torsion. Figure 8 shows the cross section dimensions of the angle and analysis model set-up. Material properties used were a modulus of elasticity of 89,660 MPa and a Poisson's ratio of 0.44. A 177.8 mm length segment was modeled as a cantilevered beam with an applied end rotation up to 100°. The line element models were meshed with 64 elements measuring 2.78 mm. At the end of the member a vertical rigid link was added from the end node to the shear center to track its position. The shell element model was defined at the centerline of the cross section and meshed with a seed size of 0.487 mm for 30 elements per leg. The nodes on the fixed end where restrained for torsion and both transverse shears. Only the 2 nodes on the tips and the corner node were restrained axially to allow the section to warp while still providing enough support to satisfy equilibrium. The same three nodes on the free end were tied to a reference point at the centroid where the end rotation was specified.

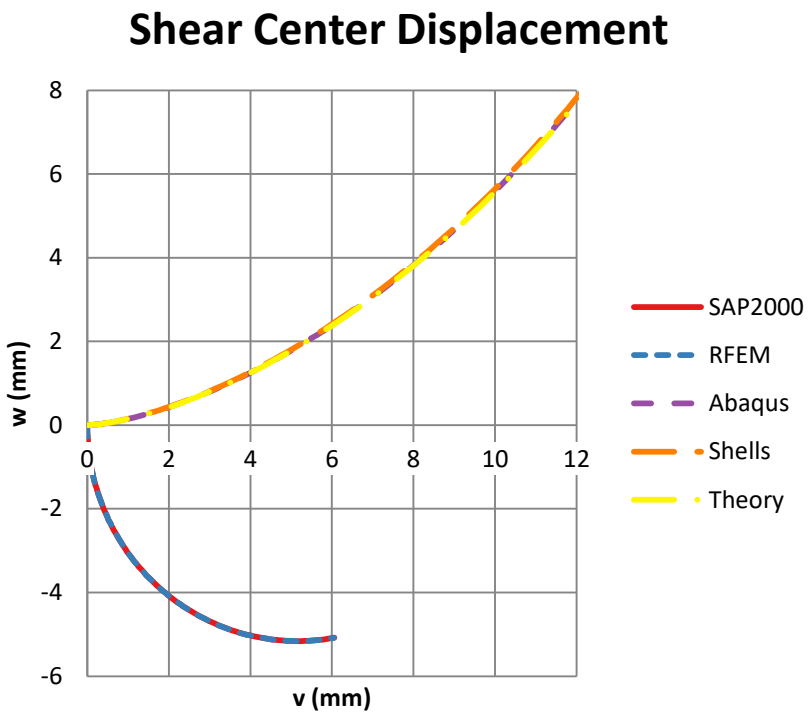

Figure 9: Shear Center Displacement of an Equal Angle Subjected to Pure Torsion

The resulting displacements from the programs considered are shown in Figure 9 in addition to the analytical solution utilizing a thin-wall approximation for $\beta_1$. The relationship with the twist of the cross section made the overall response quite nonlinear. While a twist of 25° would

already be significantly larger than expected in many structural applications, the first 25° of twist only captures the first 1 mm of weak axis displacement in the plotted solution. Since the lateral displacements correspond to a specific rotation, Table 4 and Table 5 were also provided for reference. The two very distinct displacement patterns were expected. The solutions from SAP2000 and RFEM are accurately displaying the result assuming a doubly symmetric section. A doubly symmetric section would have the rotation centered at the centroid which would be concentric with the shear center. As a result, the plot is showing the circular path around the centroid with the first movement in the *w* direction. If the programs were centering the rotation about the shear center, the graph of displacement would be expected to consist of a dot for this problem without the inclusion of warping in the analysis to cause the lateral deformations. The analysis results when including warping and singly symmetric section properties matched well with the analytical solution. The requirement that the section has no net axial force caused a resulting internal moment to counter the normal stresses due to the elongation from the member experiencing helical strains which translated to the movement of the shear center.

Table 4: Error in *v*-Displacement of Shear Center of Equal Angle in Pure Torsion

| Rotation | 5° | 10° | 25° | 50° | 75° | 100° |
|---|---|---|---|---|---|---|
| Reference (mm) | 0.039 | 0.157 | 0.968 | 3.690 | 7.657 | 12.125 |
| | | | | | | |
| SAP2000 | -50.1% | -50.1% | -50.1% | -50.1% | -50.1% | -50.1% |
| RFEM | -50.1% | -50.1% | -50.1% | -50.1% | -50.1% | -50.1% |
| ABAQUS | 0.00% | 0.00% | 0.02% | 0.08% | 0.16% | 0.26% |
| Shells | 0.48% | 0.47% | 0.47% | 0.48% | 0.38% | 0.05% |

Table 5: Error in *w*-Displacement of Shear Center of Equal Angle in Pure Torsion

| Rotation | 5° | 10° | 25° | 50° | 75° | 100° |
|---|---|---|---|---|---|---|
| Reference (mm) | 0.001 | 0.009 | 0.142 | 1.101 | 3.544 | 7.857 |
| | | | | | | |
| SAP2000 | -39416% | -9903% | -1639% | -459% | -241% | -165% |
| RFEM | -39415% | -9902% | -1639% | -459% | -241% | -165% |
| ABAQUS | 0.30% | 0.31% | 0.34% | 0.44% | 0.60% | 0.78% |
| Shells | -7.35% | 1.41% | 2.61% | 2.31% | 2.00% | 1.52% |

### *3.2 Stability of a Lipped Channel*

A lipped channel section was evaluated under a series of different loading combinations to identify the buckling responses that could be calculated when evaluating with different analysis methods. The full buckling response of a thin-walled section would be influenced by flexural and torsional buckling based on the full length of the member as well as the local and distortional buckling. CUFSM (Li & Schafer 2010) is able to account for flexural, torsional, local, and distortional buckling modes and find the accurate buckling load for a member. However, the typical line element used in structural analysis is not capable of including the local and distortional buckling values. Instead, a solution to the buckling problem considering only flexural and torsional buckling discussed by Cheng et al. (2013) was utilized as the reference solution for this comparison.

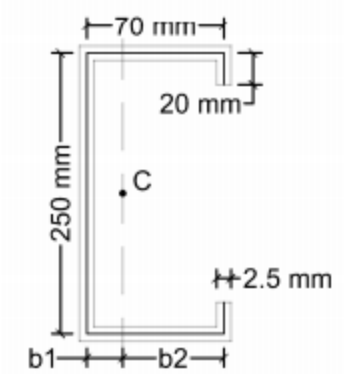

Figure 10: Lipped Channel Dimensions

Figure 10 shows the lipped channel section considered. The channel was evaluated as a simply supported member with the ends free to warp using eight different loading combinations at two different member lengths, 3 m and 12 m. The member was subjected to uniform axial compression ($P$), a strong axis moment ($M_s$), and a weak axis moment causing compression at the lips on the channel ($M_w$). The loads applied were normalized to the first values to cause compressive yielding. Additionally, a combined buckling response was evaluated using the load combinations of $0.5P+0.5M_s$, $0.5P+0.5M_w$, $0.5P+0.25M_s+0.25M_w$, $0.5M_s+0.5M_w$, and $0.5M_s-0.5 \bullet b_2/b_1 \bullet M_w$. The final load case included extra dimensional information to adjust the applied weak axis moment to represent the first compressive yield at the web instead of the lip. The member was evaluated for each load case to find a critical load factor using CUFSM and Cheng's approach with the results summarized in Table 6. The results are nearly identical at long member lengths where flexural and torsional effects dominate the buckling capacity. At shorter lengths, there was some variation in the results due to the influence of local and distortional effects with the largest occurring in case 8 where local and distortional effects would be controlling the buckling capacity.

Table 6: Lipped Channel Buckling Factors

| Case | | 1 | 2 | 3 | 4 | 5 | 6 | 7 | 8 |
|---|---|---|---|---|---|---|---|---|---|
| Method | L (m) | P | Ms | Mw | 0.5P + 0.5Ms | 0.5P + 0.5Mw | 0.5P + 0.25Ms + 0.25Mw | 0.5Ms + 0.5Mw | 0.5 Ms – 0.5•b2/b1•Mw |
| CUFSM | N/A[1] | 0.303 | 1.400 | 2.085 | 0.587 | 0.917 | 0.721 | 1.800 | 0.592 |
| CUFSM | 3 | 0.411 | 0.663 | 1.633 | 0.530 | 0.727 | 0.632 | 1.089 | 1.988 |
| CUFSM | 12 | 0.027 | 0.062 | 0.228 | 0.044 | 0.054 | 0.050 | 0.109 | 0.179 |
| Cheng | 3 | 0.431 | 0.670 | 1.676 | 0.538 | 0.731 | 0.640 | 1.101 | 2.284 |
| Cheng | 12 | 0.027 | 0.062 | 0.228 | 0.044 | 0.054 | 0.050 | 0.109 | 0.180 |

1. This row provides the critical local and/or distortional buckling value. Due to the variation in the length at which this result occurs for each loading case, no length values were provided.

The same analysis was repeated with each structural analysis program. A simply supported member was subdivided into 64 line elements with the ends restrained for torsion and free to warp. The members were loaded at both ends with equal and opposite magnitudes for the appropriate combination based on the yield loads calculated from CUFSM. The solutions from MASTAN2 and Abaqus were obtained from an eigenvalue buckling analysis. The inclusion of RFEM allowed for the use of a module that could complete an eigenvalue buckling analysis with the consideration of warping on a double symmetric element. Since not all structural analysis

programs can complete an eigenvalue buckling analysis, the results from SAP2000 were found by incrementally increasing the applied load and observing the displacement of the center of the element. For this method to capture buckling, the model in SAP2000 was altered with a small initial eccentricity of L/2000 towards the web to provide an initial perturbation. Failure was defined at the maximum applied load when the model failed to converge or when the incremental displacement was found to be at least 1000 times the initial time step displacement in a stable post buckling result.

The shell element model was defined based on the mid-surface of all sections. The shell was meshed with a seed size of 2.5 mm resulting in 172 elements around the perimeter of the channel. The requirement that the end of the channel was free to warp required that the end of the member could not be tied together. As a result, the load was applied directly to the shell elements as distributed edge loads. The application of this load type could be nonconservative in a nonlinear analysis; however, the buckling analysis was based on a linear initial condition and no change in the direction of the loading was considered.

Table 7: Error in Buckling Factor to Cheng Solution with L=3m

| Program/Case | 1 | 2 | 3 | 4 | 5 | 6 | 7 | 8 |
|---|---|---|---|---|---|---|---|---|
| SAP2000 | -2.9% | -54.3% | N/A | -48.0% | 11.9% | -30.1% | -66.5% | -80.1% |
| RFEM | -0.9% | -1.2% | 7157% | -1.2% | 16.7% | 7.9% | 46.2% | -66.6% |
| MASTAN2 | 0.0% | 0.0% | 0.1% | 0.0% | 1.0% | 0.2% | 0.0% | 0.0% |
| ABAQUS | -0.2% | -0.1% | -12.7% | -0.2% | 17.6% | 4.8% | 21.5% | -41.9% |
| Shells | -30.9% | -1.1% | -6.7% | -1.4% | -1.4% | -1.5% | -2.0% | -75.5% |

Table 8: Error in Buckling Factor to Cheng Solution with L=12m

| Program/Case | 1 | 2 | 3 | 4 | 5 | 6 | 7 | 8 |
|---|---|---|---|---|---|---|---|---|
| SAP2000 | -3.4% | -28.7% | N/A | -16.1% | -2.5% | -7.6% | -4.8% | -38.1% |
| RFEM | 0.0% | -0.4% | 3447% | -0.2% | 0.0% | 1.0% | 29.8% | -52.9% |
| MASTAN2 | 0.0% | 0.0% | 0.1% | 0.0% | 0.0% | 0.0% | 0.0% | 0.0% |
| ABAQUS | 0.0% | 0.0% | -40.3% | 0.0% | 0.0% | 0.6% | 14.1% | -31.2% |
| Shells | -0.1% | -0.5% | -4.7% | -0.3% | -0.1% | -0.2% | -1.1% | 1.0% |

The results summarized in Tables 7 and Table 8 indicate that it is not possible to capture all buckling responses when excluding warping and treating the member as doubly symmetric. SAP2000 was capable of obtaining reasonably accurate results when the mode was flexural buckling, but failed when a torsional response was expected. The weak axis moment load case that did not provide a result was not unexpected. Since the initial model imperfection was parallel to the deformation from the applied load, the model remained in a perfectly stable configuration. Additional evaluations with initial imperfections in a different orientation could have been performed; however, the results were left to highlight the challenges with this analysis type. The addition of warping to a doubly symmetric element with RFEM better captured the torsional buckling modes, but errors were still substantial for some of the failure modes with weak axis loading.

The remaining programs included both warping and nonsymmetric behavior and were able to better calculate the buckling behavior. The analysis from MASTAN2 incorporated that information to match very well with the anticipated solution. The Abaqus line elements performed better than the doubly symmetric element with warping at capturing the results, but

discrepancies where still found when including weak axis moment. These errors were attributed largely to the limitations of the analysis type used. The use of a linear perturbation buckling analysis is recommended for situations where the solution is relatively linear and elastic. The buckling mode for weak axis buckling exhibited significant nonlinear torsion at failure as shown in Figure 11. A nonlinear buckling analysis similar to the process used with SAP2000 could have possibly addressed these issues but was not completed. The shell element modeling accurately captured the global features, but also captured local and distortional buckling which led to errors due to the methodology used in this study. It was observed that the significant errors identified in the shell element modeling results actually match well with the local and distortional buckling limits identified by CUFSM and provided in Table 6.

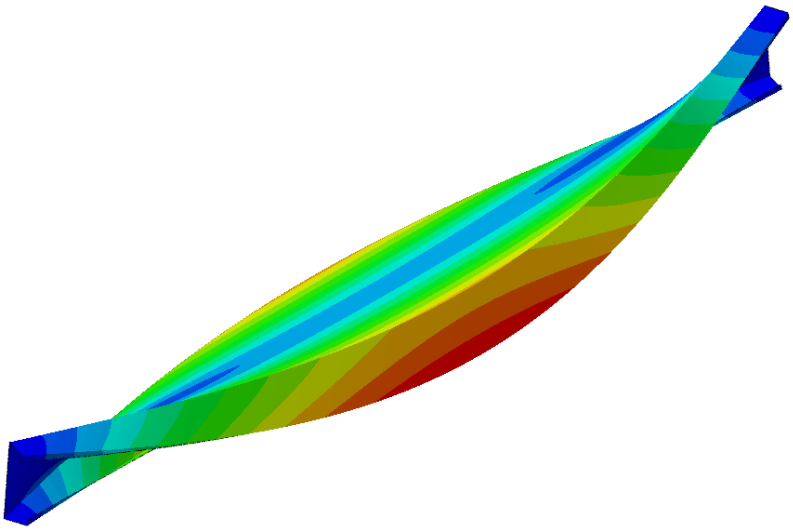

Figure 11: Channel Buckling Under Weak Axis Moment. Displacements x300

*3.3 Simply Supported Z-Section*

A series of simply supported Z-section beams were considered. Moore (1986) provided reference to two previous sets of experimental results comprising three tests for an unrestrained Z-section member as well as a nonlinear beam theory evaluation of the same tests. Figure 12 shows the geometry and loading configuration for the members considered. The first case was an unequal flange Z-section subjected to a single point load at midspan with a length of 2,000 mm. The

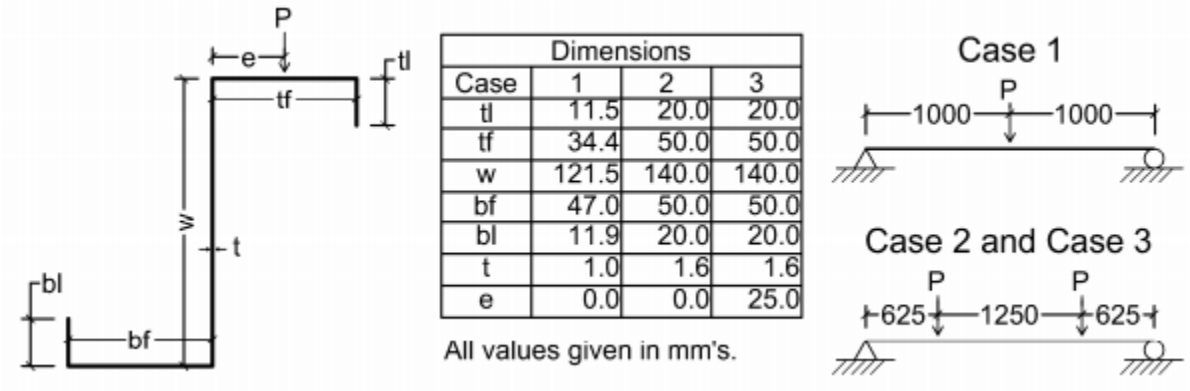


| Dimensions | | | |
|---|---|---|---|
| Case | 1 | 2 | 3 |
| tl | 11.5 | 20.0 | 20.0 |
| tf | 34.4 | 50.0 | 50.0 |
| w | 121.5 | 140.0 | 140.0 |
| bf | 47.0 | 50.0 | 50.0 |
| bl | 11.9 | 20.0 | 20.0 |
| t | 1.0 | 1.6 | 1.6 |
| e | 0.0 | 0.0 | 25.0 |

All values given in mm's.




Figure 12: Z-Section Dimensions and Loading Configuration

other two experiments subjected an equal flange Z-section to equal point loads at the quarter points on a beam of total length 2,500 mm. The variation between these two experiments was the location along the top flange where the load was applied.

The problems described by Moore (1986) provided the majority of the necessary information to complete a comparison analysis, but a few details were not provided including the modulus of elasticity and how the simple support was obtained to restrain torsion but allow warping. Without this information, this experimental data was used to verify the general accuracy of the shell element modeling procedure based on the response observed. The shell element models were created using the mid-surface of the Z-sections. The ends were modeled with all end nodes restrained for translation in the vertical and lateral directions as well as torsional rotations. The axial restraint for stability was applied via a rigid tie over the height of the web with the reference node being axially restrained to distribute any reaction and still allow the flanges to warp. The point loads were applied to a single node on the cross section, but that cross section had the web and the top flange of the Z-section tied together to distribute the load to the full member better. The choice of these two segments was to be consistent between all three models and to allow for warping between the top and bottom flange to occur. The cross section was meshed with a seed size of 1 mm in all directions. The modulus of elasticity was set to 203 GPa and the Poisson's ratio to 0.3 based on typical AISI values for all models.

The results indicated that the shell element model was capable of capturing the expected nonlinear deformations. Figure 13 contains the vertical deflection at midspan results from Case 1 as an example. The current shell element analysis was exhibiting a similar deformation response compared to experimental results and other reference theory where the shell results were consistently slightly larger suggesting that the previous analyses might have used a higher modulus of elasticity. The greatest discrepancies occurred in Case 3 with the eccentrically applied loading. For example, Figure 14 highlights the vertical displacement where the shell element analysis captures the decreasing stiffness of the member, but has a different magnitude. Other minor discrepancies existed, but without additional details of the original set-up it was determined that the shell element analysis results were reasonable to use as a reference.

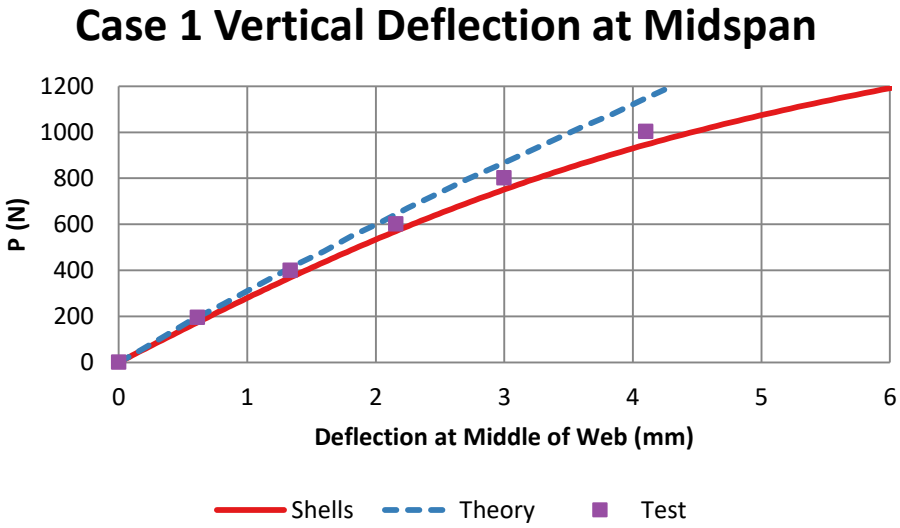


Figure 13: Vertical Deflection at the Middle of Web at Midspan of Case 1

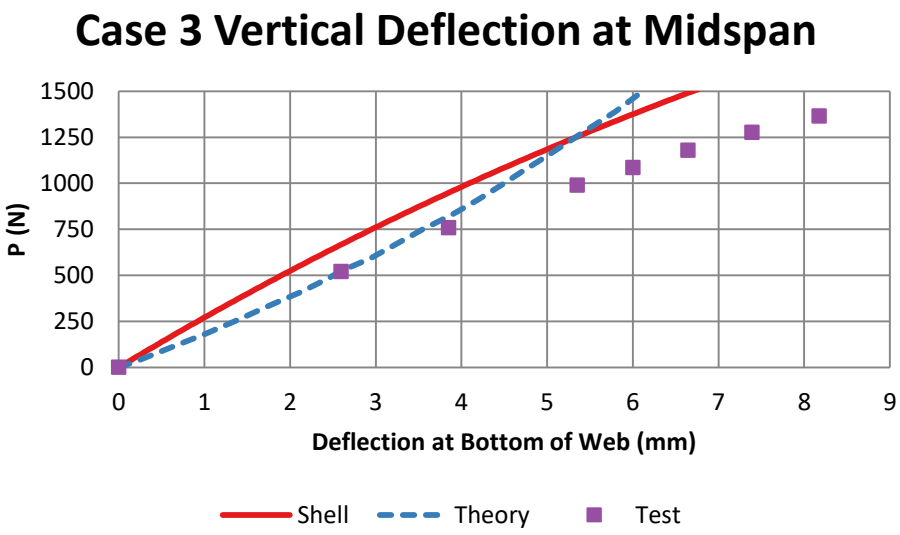


Figure 14: Vertical Deflection at the Bottom of the Web of Case 3

The line element analysis was run with an initially straight member meshed into 64 elements. The line element analyses considered two alternatives for applying the load as a result since both the experimental set-up and the shell element model had accounted for the loading being applied to the top flange. The models were analyzed with the load applied to the centroid with any torsion from the load starting offset from the shear center and a second case where the load was applied to a node at the appropriate location connected to the centroid via a rigid link. The vertical deflections from Case 2 using both loading methods are shown in Figure 15 and Figure 16. For clarity, only one set of results is shown for a doubly symmetric analysis without warping and another for an analysis without those assumptions since the corresponding results were visually similar. When using the doubly symmetric element, the vertical displacement was consistently found to be conservative. The increased rotation of the section resulted in more of the load being resisted by the weak axis bending of the section. As a result, applying the load at the centroid provided a better approximation of the actual displacement as the missed additional torsional moment was compensated for by the increased rotation that occurs due to not including the warping stiffness. This was in contrast with the results from the non-doubly symmetric analyses. The amount of twist of the section corresponded well with the shell element model. The inclusion of the offset link allowed for the analysis to capture the additional torsion that was applied to the beam as it rotated due to the load not being applied at the shear center of the cross section. As a result, any following tabulated results follow the convention that the SAP2000 and RFEM results were from a model with an equivalent loading applied to the centroid and the MASTAN2 and Abaqus results were from a model with the loading applied via a rigid link such as in Table 9 which summarizes the proceeding figures.

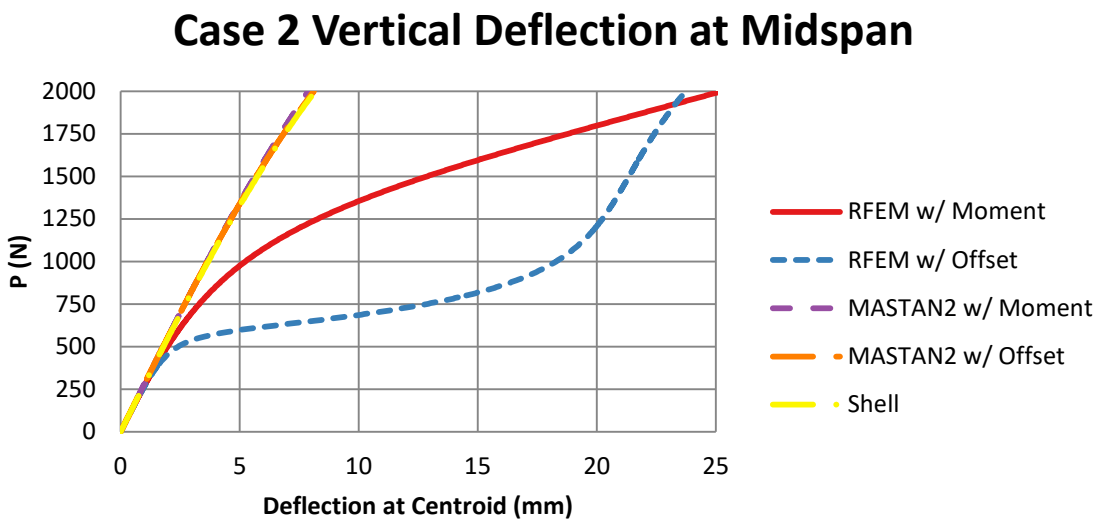


Figure 15: Vertical Deflection of the Centroid at Midspan of Case 2

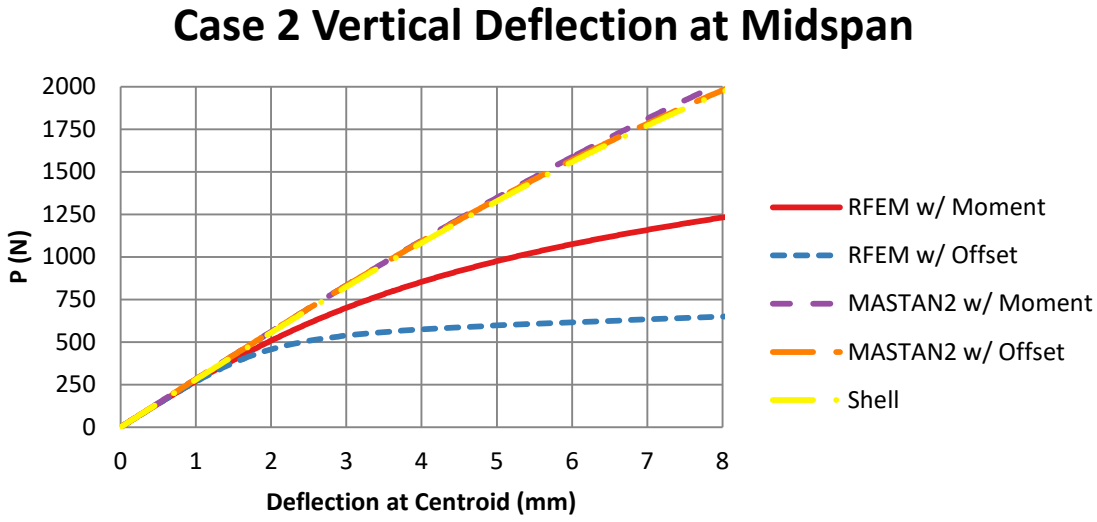


Figure 16: Close-up of Vertical Deflection of the Centroid at Midspan of Case 2

Table 9: Vertical Deflection of the Centroid at Midspan of Case 2

| Program | SAP2000 | RFEM | MASTAN2 | ABAQUS | Shells |
|---|---|---|---|---|---|
| *P* (N) | Error | | | | Reference (mm) |
| 250 | 2.77% | 2.99% | -1.02% | -0.49% | 0.895 |
| 500 | 8.87% | 9.13% | -1.01% | -0.50% | 1.800 |
| 750 | 20.9% | 21.1% | -0.99% | -0.51% | 2.723 |
| 1000 | 42.1% | 42.4% | -0.97% | -0.54% | 3.679 |
| 1250 | 76.7% | 77.0% | -0.93% | -0.60% | 4.680 |
| 1500 | 124% | 124% | -0.86% | -0.70% | 5.745 |
| 2000 | 184% | 209% | -0.61% | -1.01% | 8.164 |

Table 10: Vertical Deflection of the Centroid at Midspan of Case 3

| Program | SAP2000 | RFEM | MASTAN2 | ABAQUS | Shells |
|---|---|---|---|---|---|
| *P* (N) | Error | | | | Reference (mm) |
| 250 | 45% | 45% | -1.01% | -0.52% | 0.926 |
| 500 | 103% | 103% | -0.87% | -0.48% | 1.928 |
| 750 | 169% | 169% | -0.64% | -0.41% | 3.022 |
| 1000 | 226% | 226% | -0.27% | -0.29% | 4.230 |
| 1250 | 260% | 260% | 0.27% | -0.10% | 5.578 |
| 1500 | 269% | 269% | 1.02% | 0.20% | 7.095 |
| 2000 | 191% | 244% | 3.30% | 1.22% | 10.78 |

Table 11: Lateral Displacement of the Centroid at Midspan of Case 2

| Program | SAP2000 | RFEM | MASTAN2 | ABAQUS | Shells |
|---|---|---|---|---|---|
| *P* (N) | Error | | | | Reference (mm) |
| 250 | 2.6% | 2.7% | 0.13% | 0.17% | 1.42 |
| 500 | 6.7% | 6.8% | 0.13% | 0.16% | 2.86 |
| 750 | 13.9% | 14.0% | 0.13% | 0.14% | 4.31 |
| 1000 | 24.1% | 24.2% | 0.13% | 0.11% | 5.80 |
| 1250 | 35.6% | 35.7% | 0.13% | 0.04% | 7.35 |
| 1500 | 43.2% | 43.3% | 0.13% | -0.05% | 8.95 |
| 2000 | 29.6% | 32.4% | 0.18% | -0.33% | 12.46 |

The application of a vertical load that did not align with the principal orientation caused deformation in both principal directions resulting in a torsional loading to exist in the equilibrium condition, even for Case 2 where no initial torque was applied. As a consequence, all three cases in all programs exhibited vertical, lateral, and torsional displacements with a small selection provided in Table 9 through Table 11. The inclusion of warping and asymmetric section properties allowed for MASTAN2 and Abaqus to accurately capture the vertical and lateral displacement of the sections. As seen by Table 10, the results of the analysis became more variable in the presence of an initial torque, but still were accurate. Assuming a doubly symmetric section without warping resulted in significantly larger displacements from SAP2000 and RFEM specifically due to the increased rotation of the element. This increased deformation was often conservative as the above tables indicate for vertical and lateral displacement; however, that was not always the case.

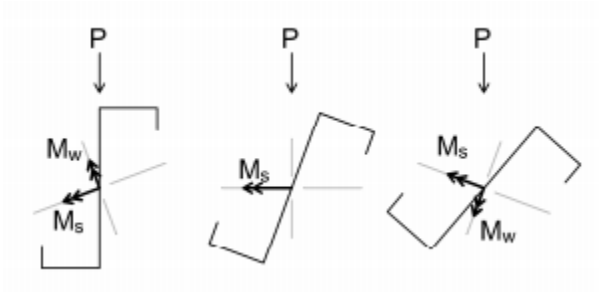


Figure 17: Principal Moments Considering Member Twist

The unconservative results observed from using a doubly symmetric analysis compared to other methods were related to the rotation of the section. While reviewing the lateral deformation results, it was noticed that the initial displacement always went in the anticipated direction in a conservative response. However as the loading was increased and the rotation of the beam increased, the lateral deformation of the beam could be observed to suddenly reverse as shown in Figure 18 for Case 3. In these problems, the additional rotation caused the applied vertical load to have a different controlling response by altering the moments experienced about the principal axes as depicted in Figure 17. The general response of the cross section to move down and to the right gradually changed as the rotation increased to the point where the section would only deflect downwards and then eventually tended to move back to the left. Without the overestimation of the rotation of the cross section, this type of behavior would not be expected to occur at low loadings. Additionally when considering the full cross section, calculations including the translations and rotation of the cross section can result in interesting situations with the displacements. While the vertical deflection from Case 1 indicated the centroid was continually deflecting downward, calculations for the location of the middle of the web do not match as shown in Table 12. This could cause a practical concern for instance if evaluating the ability for a tie rod to pass through the center of the member and result in a hole being incorrectly located or sized.

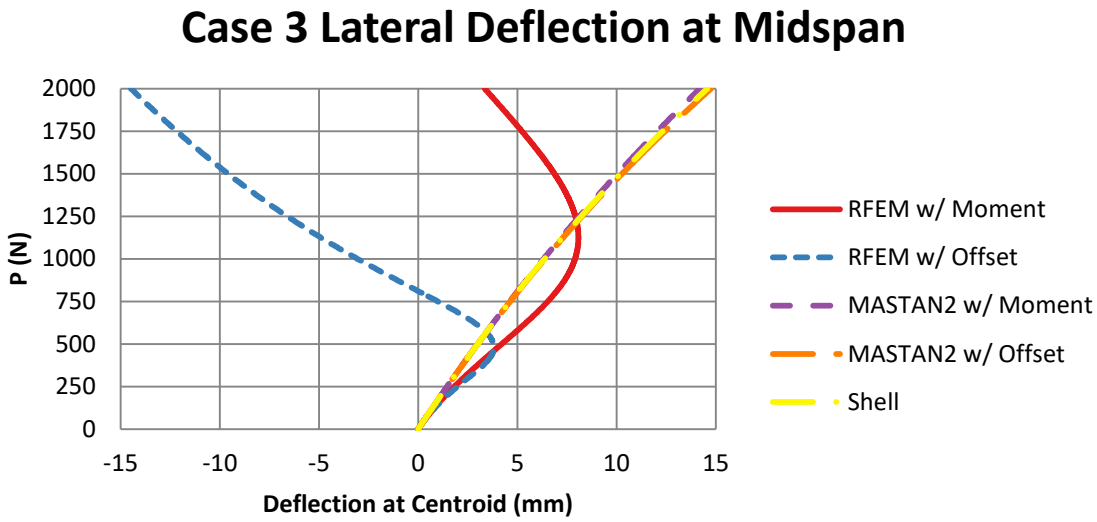


Figure 18: Lateral Displacement of Centroid at Midspan from Case 3

Table 12: Calculated Vertical Displacement at Middle of Web from Case 1

| Program | SAP2000 | RFEM | MASTAN2 | ABAQUS | Shells |
|---|---|---|---|---|---|
| *P* (N) | Displacement (mm) | | | | |
| 200 | 0.890 | 0.891 | 0.668 | 0.705 | 0.688 |
| 400 | 1.781 | 1.789 | 1.362 | 1.446 | 1.447 |
| 600 | 2.113 | 2.124 | 2.116 | 2.267 | 2.286 |
| 800 | 1.123 | 1.148 | 2.970 | 3.208 | 3.227 |
| 1000 | -[1] | -0.307 | 4.030 | 4.365 | 4.443 |
| 1200 | - | -1.016 | 5.535 | 5.934 | 6.082 |
| 1400 | - | -[2] | 8.004 | 8.264 | 8.332 |

1. SAP2000 failed to converge at 900 N
2. RFEM failed to converge at 1200 N

## 4. System Modeling

While the analysis of an individual member is an important component of design, many structures consist of a system of members that support the applied load together. The loading is distributed to elements in a system based on the requirement of statics as well as compatibility and the relative stiffness of the various components. The consideration of non-doubly symmetric sections introduces additional displacements and complicates the transfer of forces between non-linear members. As a result, this project started a series of evaluations on a portal frame to compare the ability of different analysis procedures to capture the appropriate behavior.

### *4.1 I-Beam Portal Frame*

The portal frames utilized for this project were based on the frames originally used by El-Zanaty et al. (1980) since the authors were not able to identify any experimental testing of non-tapered mono-symmetric I-beams in a system. Rosson (2017) and Ziemian and McGuire (2002) have used frames based on El-Zanaty's initial work to validate various inelastic analysis results. While this current project is limited to an elastic analysis, the general behavior of the frame was preferred. It was desirable to work with a frame that exhibited minimal force redistribution and exhibited compact behavior as to minimize the impacts of global axial buckling and lateral torsional buckling. The altered frame is shown below in Figure 19.

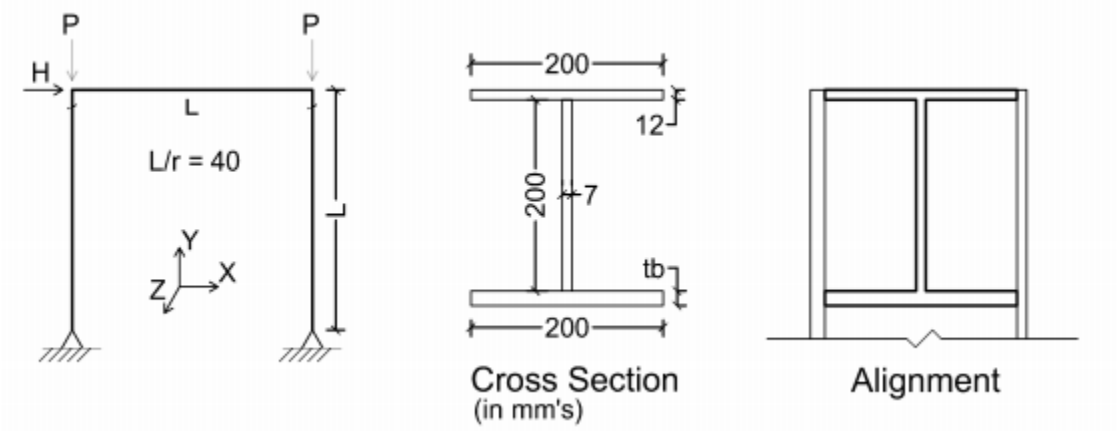


Figure 19: Modified Portal Frame for Mono-Symmetric System

The modified portal frame maintained the original dimensions of equal length columns and beams with a ratio of $L/r = 40$ and used the cross section shown in Figure 19. The variable flange thickness, $t_b$, was evaluated with thicknesses of 12 mm, 18 mm, and 24 mm to vary the amount of mono-symmetry from a control doubly symmetric cross section. Similar to the analysis completed by Ziemian and McGuire (2002), the columns were oriented in weak axis bending with the variable flange in the positive Z-direction while the beam was oriented in strong axis bending with the variable flange down. This combination of weak and major axis bending caused the frame to exhibit out of plane movements without an initial deformation when subjected to the lateral loading, *H*. The beam and column were modeled such that the beam was always located within the depth of the column. The support reactions for the frame were complicated due to the addition of out of plane effects. The ends of all members were treated as fixed for warping. The top corners at the column centroid were supported out of plane with a roller in the Z-direction to provide stability and simulate a connecting brace. The bottom supports were first treated as pinned in all directions, but a second set of evaluations was completed with this support also fixed for twist in the Y-direction controlling torsion in the column.

The steel was modeled in accordance with the Direct Analysis Method provisions reducing stiffness of sections by using 0.8E for the analysis. Prior to any adjustment the modulus of elasticity was taken as 200 GPa and the Poisson's ratio was set to 0.3. The portal frames were evaluated in each program with an increasing lateral load, *H*, up to 240 kN applied to the centroid of the beam with no vertical load, *P*, applied. The resulting axial demand in either column did not exceed the limit to require applying the additional $\tau_b$ stiffness modification per the Direct Analysis Method. No initial imperfection was included in the models as the applied lateral load caused the frame to begin to sway.

*4.2 Modeling Configuration*

Similar to the previous examples, a shell element analysis was to be used as a baseline model for comparison. The 3 identical I-beam members were modeled individually using methods mentioned previously. The model was meshed to have 100 elements across the flange using a seed mesh size of 2 mm. The requirement that the ends of the members be fixed for warping allowed for the use of a rigid tie at the end of each member to apply boundary conditions, member to member connections, and loadings via a single node located at the centroid of the member. This modeling decision excluded the modeling of the actual deformation of the column-beam joint which allowed for a better comparison to the line element models which would not be able to capture that deformation as any load in the beam cross section would be transferred to the full cross section of the column.

The line elements models were created with 3 full length members meshed into 50 elements giving elements approximately 41 mm long. The requirement that the beam was located within the depth of the column caused the centroids of the column and beam to not be aligned. It was decided to use a single horizontal rigid link to connect the centroids of those members in SAP2000, RFEM, and MASTAN2 to avoid the use of member offsets in the definition of the cross section. A rigid tie was again used in Abaqus to connect the members, but since the cross sections where modeled with the shear center as the reference location additional nodes for the centroid locations were included in the models as the location to provide loading and support reactions. A similar centroid node connection was included at all locations of interest to compare displacements at the centroid.

*4.3 Initial Results*

The evaluation of these six frames found that the overall lateral deformation, in plane shear reactions, and vertical reactions had minimal variation based on the type of analysis completed. An example of the lateral deformation is shown in Figure 20. However, this trend did not continue to the out of plane responses. The inclusion of a lateral offset in the model did cause the doubly symmetric analyses to exhibit some similar behavior, but it was found to not be consistent with an analysis that accounted for the asymmetry of the section. Observations of the Z-direction displacement at the center of the column found that it typically was in the correct direction but varied in magnitude. Results for the displacement were both underestimated and overestimated with one example shown in Figure 21 for the right column with $t_b$ = 18 mm.

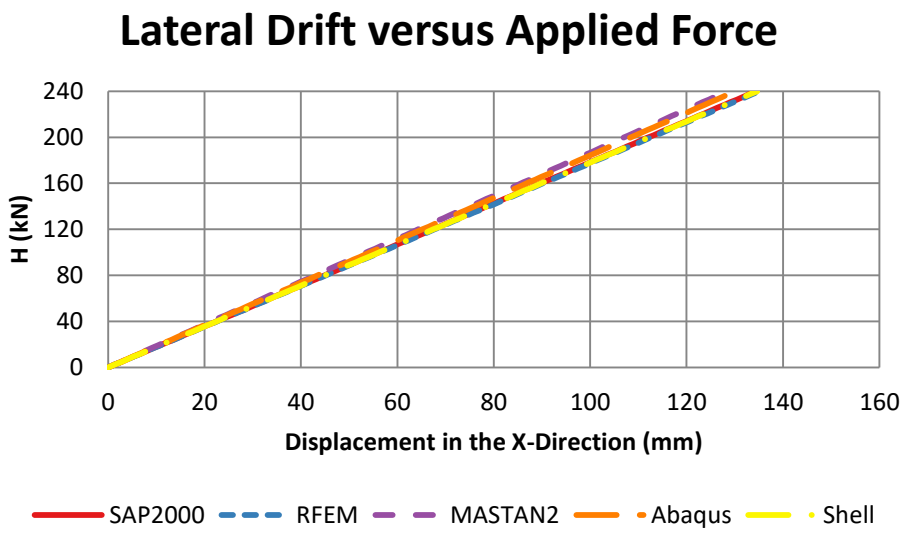


Figure 20: Lateral Deformation of Frame without Torsion Restraint and $t_b$ = 18mm

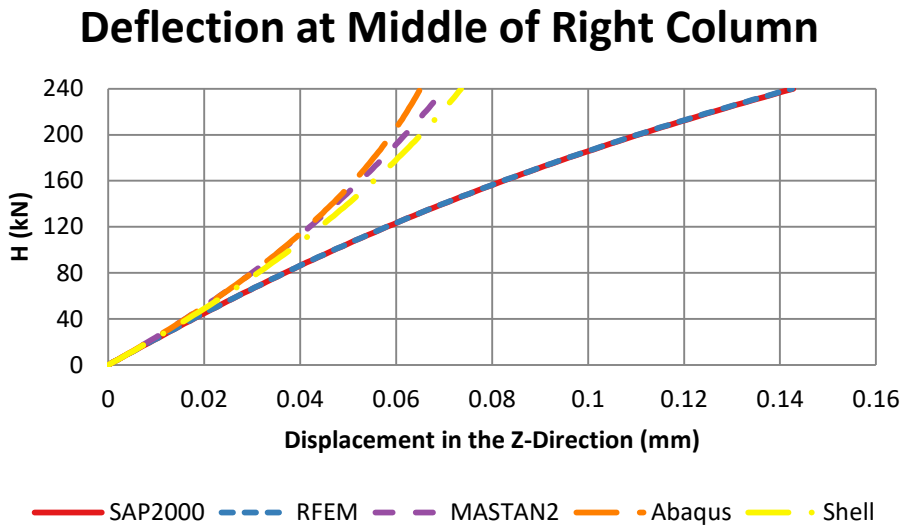


Figure 21: Out of Plane Displacement of Frame without Torsion Restraint and $t_b$ = 18mm

The twist responses of the columns were also quite different. While the singly symmetric analysis included the effects of warping and as such would have been stiffer against torsion, it was observed that the columns in the doubly symmetric analyses were rotating less as shown in Figure 22. The inclusion of the non-doubly symmetric section properties and shear center information were causing more displacement than the soft torsional response due to ignoring warping unlike most of the previous single member example problems. When the base of the column was constrained for twist, the difference became more noticeable. The moment reaction that developed at the base was found to often be in the opposite direction in addition to being significantly underestimated as shown in Figure 23. The lateral support at the top of the frame was found to be similar while the base of the frames were free to twist, but the restraint of the bottom support reaction caused a drastic variation between the analysis options as indicated in

Figure 24. The additional torsional restraint limited the movement of the column in the doubly symmetric analysis causing the lateral reactions to stay small in contrast to the non-symmetric analysis which still had to resist twisting effects increasing the reactions.

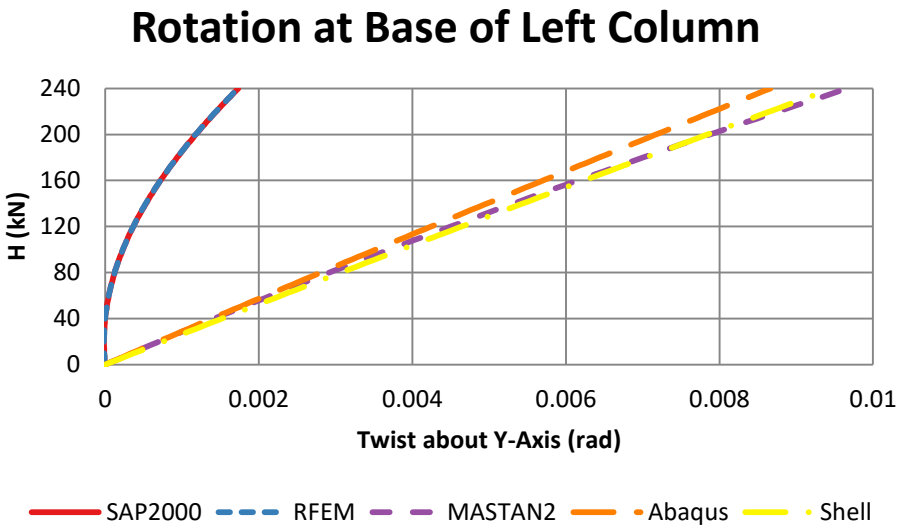


Note: SAP2000 and RFEM exhibit slightly negative rotations below 40 kN which were not shown for clarity.

Figure 22: Base Rotation of Left Column without Torsion Restraint and $t_b$ = 24 mm

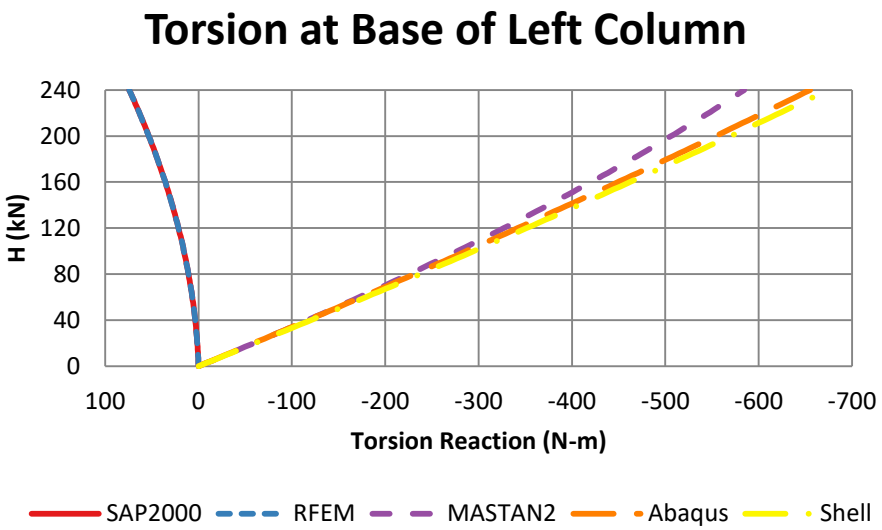


Figure 23: Torsion Reaction of Right Column with Torsion Restraint and $t_b$ = 24 mm

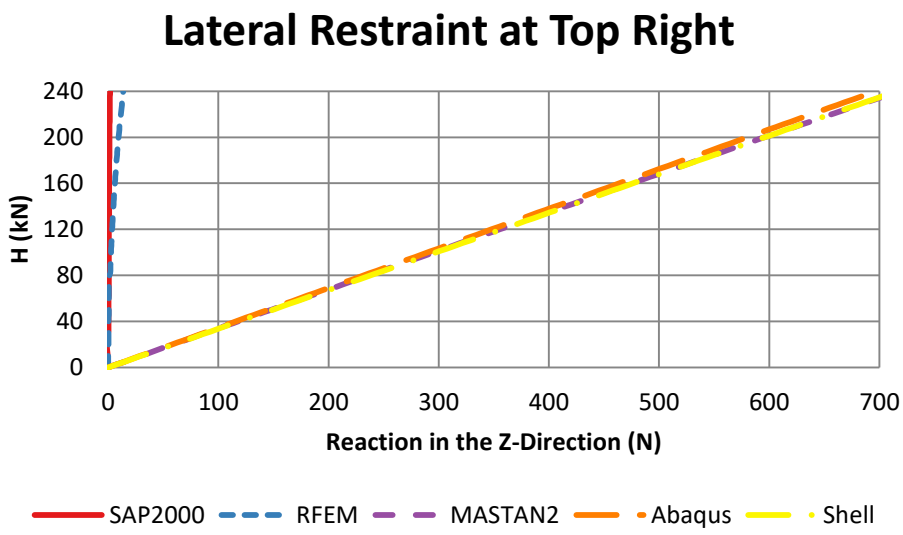


Figure 24: Upper Left Corner Lateral Support of Frame with Torsion Restraint and $t_b$ = 24 mm

*4.4 Future Work*

Future work in this project consists of two major components. The first step will be the continued evaluation of the frame system described above. The expanded work will include the addition of axial loading as well as other lengths to introduce more stability effects to the analysis. The second component will be the evaluation of a few cold-formed steel systems. Modeling comparison will be done on the experimental evaluations completed on single channel portal frames. Additional evaluations will be completed on metal roof systems to see the potential variation in the load sharing abilities.

**5. Discussion**

The analysis of non-doubly symmetric sections is sensitive to the inclusion of twisting effects that are not required as part of the Direct Analysis Method. The specification indicates that a second order analysis shall be completed highlighting the inclusion of *P-δ* and *P-Δ* effects. This definition works well when using members confined to a single plane; however, it has limitations when the analysis fails to meet that condition. If the engineer focuses specifically on the evaluation of *P-δ* and *P-Δ* effects as completing a second order analysis, it is possible to miss a situation where equilibrium on the deformed shape causes the variations. Using Case 2 of the equal flange Z-section from Section 3.3 as an example, the beam is subjected to only transverse loading. The member has no axial force when evaluating a first order analysis meaning if the engineer only considers the evaluation of *P-δ* and *P-Δ* effects as a second order analysis, they would assume that the first order analysis was an acceptable final solution. Proceeding with that logic, the applied vertical load which was not aligned with a single principal axis of the cross section would result in an unsymmetric bending analysis with a solution of deflections of 7.1 mm vertically and 11.4 mm to the right. However, the application of equilibrium on the deformed member introduces a variable torsional load along the length of the member similar to the initial imperfection required by the Advanced Analysis Method. The inclusion of torsion and the updated evaluation of equilibrium including the altered orientation of the cross section resulted in deflections of 25.3 mm vertically and 16.5 mm to the right when working with a doubly

symmetric analysis method without warping. If it is acceptable to not consider torsional effects in the analysis, this significantly increased displacement would have been missed.

The inclusion of twist effects for non-doubly symmetric sections is a complicated issue. In addition to the complications with evaluating a member where the cross section is now rotating through three dimensions, the components of the torsional response included can vary. A complete evaluation of a non-doubly symmetric section under twist would include warping effects as part of a non-linear torsion in addition to the twist of the section being centered on the shear center instead of the centroid of the cross section. As was observed in the equal angle twist problem from Section 3.1, the complete evaluation of twist is quite different from the simplified assumptions. Even when the shear center and centroid are concentric, the increased stiffness from warping considerations cause the second order twist effects to be transformed drastically. Returning to Case 2 from Section 3.3 where warping was not considered, the second order deflections drastically overestimated the vertical deformation at more than twice the expected value due to the cross section rotating which orients it to experience bending in a different direction. The addition of warping considerations and non-doubly symmetric effects in the structural analysis were able to properly account for the rotation to the member. In many applications, the results from an analysis ignoring warping were found to be conservative; however that was not always the situation. It was observed that excessive rotations could cause alteration of the expected deflection path by altering the relationship of the applied forces to the principal axis as illustrated in Figure 17. Once the member reached this level of rotation, the analysis experienced an increase in stiffness for vertical displacement and the value of rotations and lateral displacement began to decrease. While this type of response could be possible in all analyses, the inclusion of warping would keep the member stiffer to torsion preventing the premature application of this behavior. As a result, it might be poignant for the engineer to consider other methods to account for the actual total stiffness of the member when working with doubly symmetric structural analysis programs that cannot include warping such as a modified torsional constant (Dowswell 2018).

The requirement of the Direct Analysis Method that the analyzed structure must be subjected to an initial imperfection helps ensure that the system experiences second order effects. If the evaluation of that frame is approaching an elastic stability limit, the frame will begin to experience decreasing stiffness and increased movement. The ability of the different analysis methods to capture these stability failures varied significantly. The base analysis that ignored warping and assumed a doubly symmetric cross section meeting the minimums of the Direct Analysis Method was only able to display flexural failures. The exclusion of a warping stiffness underestimated the strength in many configurations. The addition of warping effects to a doubly symmetric analysis added the ability to identify torsional responses which helped to better match buckling failures including moments. However, neither of these methods could accurately capture all buckling responses of non-doubly symmetric sections where the capacity is influenced also by asymmetric cross section properties including the nonconcentric shear center and centroid. For example, the buckling of the lipped channel buckling from weak axis moment was not possible without the inclusion of singly symmetric properties as the previous methods were not able to identify a way that the section could become unstable. The inclusion of the additional cross section properties allowed for the analysis procedure to capture more buckling analysis modes at the accurate critical loading.

The evaluation of these systems as part of the Direct Analysis Method requires the consideration of all flexural, shear, and axial member deformations. The inclusion of non-doubly symmetric sections adds the additional loading effects due to the nonconcentric shear center and centroid. In a typical doubly symmetric connection, the shear and axial forces are simply transferred from one member to the next such as an axial force in the vertical column of the portal frame becomes the shear in the horizontal beam. However, in non-doubly symmetric sections where the centroid and shear center are nonconcentric there is a complication that this transfer of force must also account for moments resulting from transverse shears not passing through the shear center while not adding unintended moments where an axial force is applied at the centroid. It is then up to the engineer's judgement as to whether to include those effects or not. Most doubly symmetric analysis programs require the user to properly adjust the models to include these additional moments. The process can be relatively straight forward when working with a single straight member. However, the use of non-doubly symmetric sections in a system can lead to challenges. Typical modeling techniques could result in moments being missed or extraneous moments being added depending on the approach taken. This analysis process would require the engineer to determine whether the analysis is adequate as completed or if it needs to be iterated to correct for the effect that could not be captured. The inclusion of shear center information in addition to centroid information for the transfer of forces between members simplifies the process.

## 6. Conclusions

Finite element models were created for a series of doubly symmetric and non-doubly symmetric problems to evaluate the results of structural analysis procedures that assumed doubly symmetric cross sections versus those that do not through the use of multiple structural analysis programs. The results of the doubly symmetric problems indicated that the methodology used in each program was capable of obtaining solutions that meet both the requirements of the Direct Analysis Method or the Advanced Analysis Method. The evaluation of the non-doubly symmetric problems illustrated the importance of the consideration of twist effects including warping, the center of twist, and second order twist effects in addition to asymmetric section properties. While the analyses completed using non-doubly symmetric information where able to often match well with the anticipated solution, the doubly symmetric structural analysis varied. Depending largely on the twist of the cross section, the doubly symmetric structural analyses were able to calculate accurate to conservative results for the main displacement response of the system, but other responses were highly variable including unconservative results. Preliminary evaluation of a portal frame indicated that using the assumption of doubly symmetric sections could result in calculating incorrect out of plane responses. Further evaluation of the portal frame problem is required to determine the significances of these differences particularly when working with a frame that will exhibit instabilities.

## Acknowledgments

The authors would like to thank Siwei Liu and his research team at Sun Yat-Sen University for their assistance with the updated MASTAN2 program.

## References

AISC. (2005). *Specification for Structural Steel Buildings ANSI/AISC 360-05*. Chicago, IL: American Institute of Steel Construction.

AISC. (2010). *Specification for Structural Steel Buildings ANSI/AISC 360-10*. Chicago, IL: American Institute of Steel Construction.

AISC. (2016). *Specification for Structural Steel Buildings ANSI/AISC 360-16*. Chicago, IL: American Institute of Steel Construction.

Akin, J. E. (2010). *Finite element analysis concepts: Via solidworks*. https://doi.org/10.1142/7785

Argyris, J. H., Hilpert, O., Malejannakis, G. A., & Scharpf, D. W. (1979). On the geometrical stiffness of a beam in space-a consistent V.W. approach. *Computer Methods in Applied Mechanics and Engineering*, *20*, 105–131. https://doi.org/10.1016/0045-7825(79)90061-6

Attard, M. M. (1984). *The Elastic Flexural-Torsional Response of Thin-Walled Open Beams*. The University of New South Wales.

Attard, M. M. (1986). Nonlinear Shortening and Bending Effect Under Pure Torque of Thin-Walled Open Beams. *Thin-Walled Structures*, *4*(3), 165–177. https://doi.org/10.1016/0263-8231(86)90001-7

Cheng, S. S., Kim, B., & Li, L. Y. (2013). Lateral-torsional buckling of cold-formed channel sections subject to combined compression and bending. *Journal of Constructional Steel Research*, *80*, 174–180. https://doi.org/10.1016/j.jcsr.2012.07.026

CSI America. (2014). "Shear Center." Last Modified April 7, 2014. https://wiki.csiamerica.com/display/kb/

CSI America. (2018). *SAP2000*. V20.1.0. Berkeley, CA: Computers & Structures, Inc.

Dassault Systems. (2015a). *Abaqus/CAE*. V6.16. Johnston, RI: Dassault Systems.

Dassault Systems. (2015b). "Abaqus 2016 Documentation." http://130.149.89.49:2080/v2016/index.html

Dlubal Software. (2012). *RFEM 5*. V5.19. Dlubal Software GmbH.

Dlubal Software. (2019). *RFEM 5 User Manual* (December 2019). Dlubal Software GmbH.

Dowswell, B. (2018). Curved Member Design. In *Design Guide 33*. Chicago, IL: American Institute of Steel Construction.

El-Zanaty, M. H., Murray, D. W., & Bjorhovde, R. (1980). *Inelastic Behavior of Multistory Steel Frames*. Edmonton, Alberta, Canada.

Gregory, M. (1960). A Non-linear Bending Effect When Certain Unsymmetrical Sections are Subjected to a Pure Torque. *Australian Journal of Applied Science*, *2*, 33–48.

Griffis, L. G., & White, D. W. (2013). Stability Design of Steel Buildings. In *Design Guide 28*. Chicago, IL: American Institute of Steel Construction.

Kaehler, R. C., White, D. W., & Kim, Y. D. (2011). Frame Design Using Web-Tapered Members. In *Design Guide 25*. Chicago, IL: American Institute of Steel Construction.

Li, Z., & Schafer, B. W. (2010). Buckling analysis of cold-formed steel members with general boundary conditions using CUFSM: Conventional and constrained finite strip methods. *20th International Specialty Conference on Cold-Formed Steel Structures - Recent Research and Developments in Cold-Formed Steel Design and Construction*.

Liu, S.-W., Gao, W. L., & Ziemian, R. D. (2019). Improved line-element formulations for the stability analysis of arbitrarily-shaped open-section beam-columns. *Thin-Walled Structures*, *144*, *November 2019*, 106290. https://doi.org/10.1016/j.tws.2019.106290

Liu, S.-W., Ziemian, R. D., Chen, L., & Chan, S.-L. (2018). Bifurcation and large-deflection analyses of thin-walled beam-columns with asymmetric open-sections. *Thin-Walled Structures*, *132*, 287–301. https://doi.org/10.1016/j.tws.2018.07.044

McGuire, W., Ziemian, R. D., & Gallagher, R. H. (2001). *Matrix Structrual Analysis* (2nd ed.).

Moore, D. B. (1986). A Non-linear Theory for the Behaviour of Thin-walled Sections Subject to Combined Bending and Torsion. *Thin-Walled Structures*, *4*(6), 449–466. https://doi.org/10.1016/0263-8231(86)90040-6

Rosson, B. T. (2017). Major and Minor Axis Stiffness Reduction of Steel Beam-Columns Under Axial Compression and Tension Conditions. *Proceedings of the Annual Stability Conference*, 1–17. San Antonio, TX: SSRC.

Spillers, W. R., Saadeghvaziri, A., & Luke, A. (1993). An Example of Three-Dimensional Frame Buckling. *Computers and Structures*, *47*(3), 483–486. https://doi.org/10.1016/0045-7949(93)90244-8

Ziemian, R. D., Batista Abreu, J. C., Denavit, M. D., & Denavit, T.-J. L. (2018). Three-Dimensional Benchmark Problems for Design by Advanced Analysis: Impact of Twist. *Journal of Structural Engineering*, *144*(12), 04018220. https://doi.org/10.1061/(asce)st.1943-541x.0002224

Ziemian, R. D., & McGuire, W. (2002). Modified Tangent Modulus Approach, A Contribution to Plastic Hinge Analysis. *Journal of Structural Engineering*, *128*(10), 1301–1307. https://doi.org/10.1061/(asce)0733-9445(2002)128:10(1301)

Ziemian, R. D., McGuire, W., & Liu, S.-W. (2019). *MASTAN2*. V5.0.2.